

Inhibitors of phosphopantetheine adenylyltransferase

Lihua Zhao^{a,*}, Nigel M. Allanson^a, Samantha P. Thomson^a, John K.F. Maclean^b,
John J. Barker^b, William U. Primrose^b, Paul D. Tyler^c, Ann Lewendon^c

^a Department of Chemistry, PanTherix Ltd, West of Scotland Science Park, Todd Campus, Glasgow G20 0XA, UK

^b Department of Structural biology, PanTherix Ltd, West of Scotland Science Park, Todd Campus, Glasgow G20 0XA, UK

^c Department of Biology, PanTherix Ltd, West of Scotland Science Park, Todd Campus, Glasgow G20 0XA, UK

Received 27 September 2002; accepted 14 December 2002

Abstract

Phosphopantetheine adenylyltransferase (PPAT) is an essential enzyme in Coenzyme A biosynthesis. Because bacterial PPAT and mammalian PPAT are dissimilar, this enzyme is an attractive antibacterial target. Based on the structure of the substrate, 4-phosphopantetheine, a dipeptide library was designed, synthesised and tested against *Escherichia coli* PPAT. The most potent inhibitor PTX040334 was co-crystallised with *E. coli* PPAT. With this structural information, a rational iterative medicinal chemistry program was initiated, aimed at increasing the number of inhibitor–enzyme interactions. A very potent and specific inhibitor, PTX042695, with an IC₅₀ of 6 nM against *E. coli* PPAT, but with no activity against porcine PPAT, was obtained.

© 2003 Éditions scientifiques et médicales Elsevier SAS. All rights reserved.

Keywords: Phosphopantetheine adenylyltransferase; Inhibitors; *E. coli*; Co-crystal structure; H-bonding; Parallel synthesis

1. Introduction

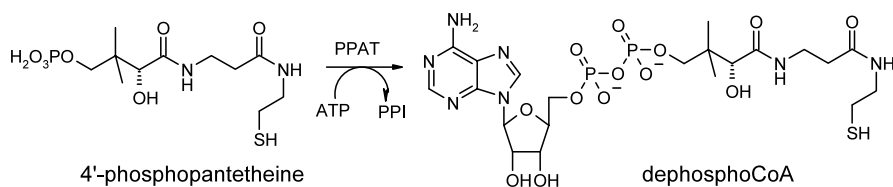
In the last decade, the emergence of both vancomycin and methicillin resistant bacteria has led to an urgent search for novel classes of antibiotics and new antimicrobial targets. Coenzyme A (CoA) is the predominant acyl group carrier in all living cells, and is required for many metabolic processes including the citric acid cycle and the synthesis of fatty acids [1]. CoA is exclusively synthesised from pantothenate, cysteine and ATP in five enzymatic steps [2,3]. Phosphopantetheine adenylyltransferase (PPAT) catalyses the penultimate step in the CoA biosynthesis pathway by transferring an adenylyl group from ATP to 4'-phosphopantetheine (4-PP), yielding dephospho-CoA and pyrophosphate (Scheme 1).

The essentiality of the PPAT gene in *Escherichia coli* has been shown by a gene knock out experiment [4].

PPAT is thus a validated antibacterial target as inhibition will reduce the intracellular levels of CoA and prevent bacterial growth. Unlike bacterial PPATs, which are monofunctional hexameric enzymes, mammalian PPAT is a dimeric enzyme and occurs as a bifunctional complex with dephospho-CoA kinase [5,6]. Comparison of PPAT sequences from different bacterial species revealed highly homology, and suggested that the selective inhibition of bacterial PPATs would be an effective therapeutic strategy for the development of new, broad spectrum antibacterial agents. We initiated the program by synthesising a substrate-based dipeptide library as potential inhibitors of *E. coli* PPAT, since parallel array synthesis and purification techniques would allow for the rapid exploration of structure-activity relationships. In addition, the existence of a high resolution crystal structure of *E. coli* PPAT complexed with 4-PP previously solved in house enabled us to target the essential substrate-binding residues—a strategy designed to minimise the development of facile target-based drug resistance in any antibacterial compound.

* Corresponding author.

E-mail address: lihua.zhao@pantherix.co.uk (L. Zhao).



Scheme 1.

2. Results and discussion

2.1. Chemistry

A dipeptide library (300 member) was designed based on the 4-PP structure, aiming at retaining the important interactions made by 4-PP, while allowing structure variations (Scheme 2).

The synthesis of this combinatorial library was performed by solid phase chemistry using IRORI autotag-100 system. Starting from Sieber amide resin, the desired amine **1** was prepared by reductive amination in four steps. Two subsequent peptide coupling reactions gave dipeptide **3**. After the removal of the Fmoc group, and acylation with R₄ groups, the molecules were cleaved from the resin to give the desired dipeptides **5** (Scheme 3). All the members of the library were analysed by LC/MS for purity and confirmation of structure.

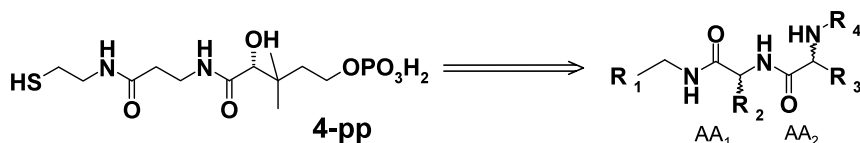
2.2. Biochemistry

The library was screened against *E. coli* PPAT using a pyrophosphate release assay [7]. IC₅₀ values of the active compounds were determined, and their selectivity measured by a counterscreen with porcine PPAT.

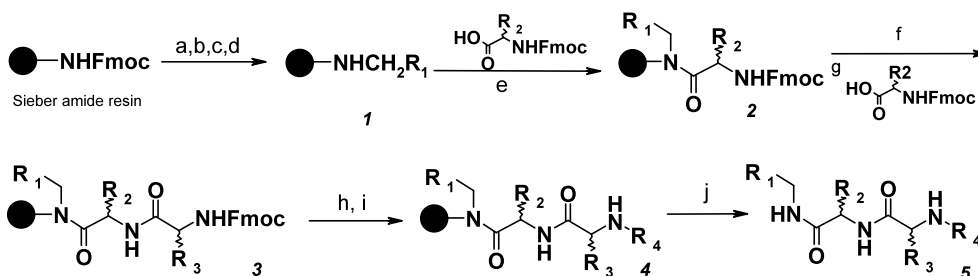
2.3. Structure-based drug design

A number of selective hits were discovered from this library. Of these, compound **6** (PTX040334) had an IC₅₀ of 0.30 μM against *E. coli* PPAT, but was inactive against porcine PPAT (Fig. 1). This inhibitor was subsequently co-crystallised with *E. coli* PPAT. In the crystal structure, the binding conformation of compound **6** is very close to the modelled global minimum conformation, with the peptide backbone and phosphoserine side-chain of **6** occupying a similar position to the corresponding groups in the substrate 4-PP (Fig. 2a). The crucial interactions with the highly conserved protein residues are conserved by the phosphate (T10, R88, Y98) and the C-terminal carbonyl (M74) of **6**, as identified in 4-PP/*E. coli* PPAT crystal structure. The Fmoc group fits snugly into a lipophilic cavity at the surface of two protein subunits, and the *D*-alanine side chain partially occupies a polar cavity which can be explored for extra H-bonding interactions.

To improve the drug-likeness of the inhibitor, the phosphoserine in **6** was first successfully replaced by a glutamic acid at the AA₂ position; this analogue had a similar IC₅₀ as **6**. Then an analogue with *D*-serine as the replacement for *D*-alanine at the AA₁ position (**7**, PTX007011) was prepared by solution phase chemistry. This had an improved IC₅₀ of 0.12 μM. **7** was also co-crystallised with *E. coli* PPAT (Figs. 1 and 2b). The



Scheme 2. A substrate-based dipeptide library.



Scheme 3. (a) 20% piperidine/DMF; (b) R₁COOH/HBTU/DIPEA, CH₂Cl₂; (c) BH₃, THF; (d) 0.06M DBU; (e) HBTU/DIPEA; (f) 20% piperidine; (g) HBTU/DIPEA; (h) 20% piperidine; (i) R₄X; (j) 2% TFA in CH₂Cl₂.

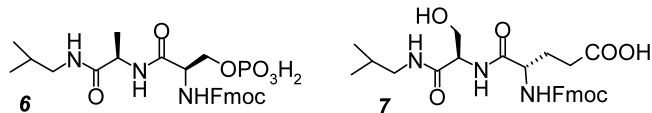


Fig. 1. Compounds 6 and 7.

crystal structure of **7**/*E. coli* PPAT showed that the serine side chain hydroxyl was present in two distinct conformations, implying that a bidentate ligand would improve the potency. The relative positions of hydrogen bond donors and acceptors within the binding pocket suggested that an imidazole ring on that position would be able to maximise favourable interactions. This compound (**8**, PTX042695) was synthesised and had an IC_{50} of 6 nM against *E. coli* PPAT (Table 1). The crystal structure of **8**/*E. coli* PPAT (not shown) confirmed that the predicted interactions had been made.

Based on the structural information, a follow-up library (700 member) was designed with the aim to

improve the potency by increasing the number of enzyme–inhibitor interactions. In addition to replacing the *D*-Serine with a bidentate ligand in AA_1 , a further consideration was to replace Fmoc with a chemically stable group with reduced molecular weight and log *P*. A selection of phenyls bearing polar substituents was investigated as potential Fmoc replacements in an effort to make extra H-bonding interactions with specific amino acids lining the Fmoc pocket. In particular, a glutamate side-chain carboxyl E134 and a serine side-chain hydroxyl S130 were targeted. The library synthesis was performed as described in Scheme 3.

2.4. SAR studies

Clear structure-activity relationships were deduced from the library. Small branched alkyl groups were best for R_1 . *D*-Amino acids or β -alanine were required for AA_1 and decreasing potency was observed in the

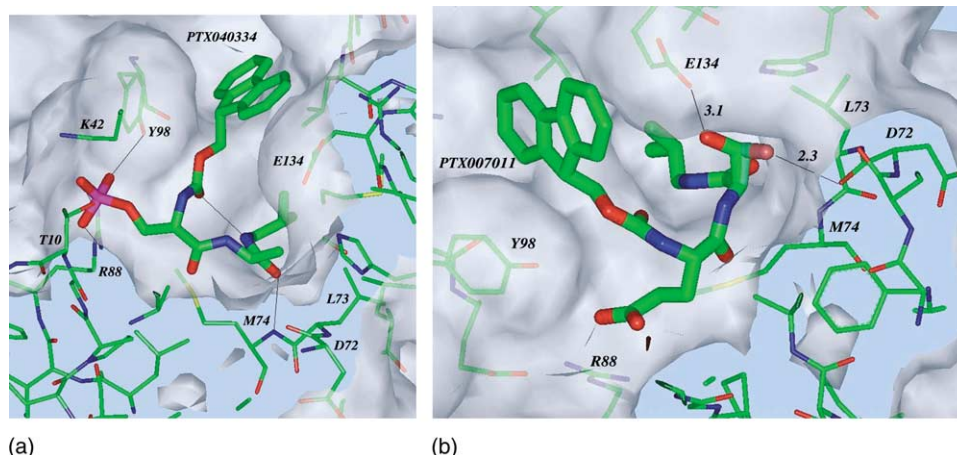
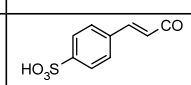
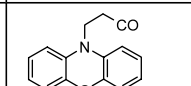
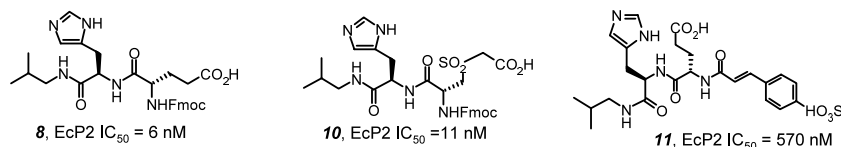
Fig. 2. Crystal structures of (a) **6**/*E. coli* PPAT; (b) overlay of two conformations of **7**/*E. coli* PPAT.

Table 1

IC_{50} values of representative dipeptides from library 2

R_1 R_2 R_3 R_4
 AA_1 AA_2

Compound d	R1	AA ₁	AA ₂	R ₄	IC ₅₀ (μM) vs <i>E. coli</i> PPAT
6	i-Pr	D-Ala	L-Phospho-Ser	Fmoc	0.30
7	i-Pr	D-Ser	L-Glu	Fmoc	0.12
8	i-Pr	D-His	L-Glu	Fmoc	0.006
9	i-Pr	D-His	D-Carboxymethyl Cys	Fmoc	0.020
10	i-Pr	D-His	D-Carboxymethyl Cys sulphone	Fmoc	0.011
11	i-Pr	D-His	L-Glu		0.57
12	i-Pr	D-His	D-Carboxymethyl Cys		0.14

Fig. 3. Compounds **8**, **10** and **11**.

following order: *D*-histidine > *D*-serine > *D*-alanine = β -alanine. For AA₂, both the *t*-butyl esters of the carboxylate side-chains and the corresponding amides were inactive, since negatively charged groups are required to make interactions with protein residues R88, T10, K42 or Y98. Fmoc remained the best substituent at R₄, although some other fused tricyclic ring systems, such as phenothiazine derivatives, were also potent (Table 1).

Two of the most potent compounds are shown in Fig. 3 along with a moderately active compound (**11**) in which the Fmoc group was replaced by a more polar substituent. The crystal structure of **11** in complex with *E. coli* PPAT was also solved which is useful for further modifications on non-Fmoc containing inhibitors. These compounds were not anti-bacterial, possibly because they lack the ability to penetrate the bacterial cell wall, or because of metabolism.

3. Conclusion

By using structure-based drug design and parallel synthesis, potent *E. coli* PPAT inhibitors were rapidly discovered, demonstrating the value of combining crystal structure information with parallel synthesis in lead optimisation. Enzyme–inhibitor co-crystal structures enabled essential substrate-contacting residues to be targeted, and two cycles of iterative design led to the discovery of a 6 nM inhibitor. A pharmacophore model developed from the crystal structure enabled identification of non-peptide inhibitors by virtual screening.

4. Experimental

4.1. Chemistry

4.1.1. General information

Fmoc–Sieber amide resin was purchased from C&N Biochem. Aminoacids were purchased from Advanced Chemtech and C&N Biochem. Peptide synthesis grade DMF was used. LC/MS analyses were performed on a Waters 2690 HPLC and a 2700 autosampler system equipped with a Micromass platform ZMD in \pm electrospray ionisation mode and a Sedex 55 evaporative light-scattering (ELS) detector. The HPLC conditions were as follows: a C18 5 μ column (5 \times 0.46 cm), eluted

over 7 min at 1 mL min^{−1} flow rate with a binary gradient. Solvent A: water and 0.05% formic acid; solvent B: methanol and 0.05% formic acid. Compound purities were assigned on the basis of ELS data. The libraries were synthesised using the IRORI autotag-100 combinatorial system in microkans containing 30 mg of resin per kan. After finishing each reaction, the kans were sequentially washed with 3 \times (DMF then MeOH), 2 \times DCM, shaking 5 min for each washing. A few beads of resin were taken and the products were cleaved from the resin by 2% TFA for LC/MS analysis to monitor the reaction after each step.

4.1.2. General procedure for Fmoc deprotection

The resin was treated with 20% piperidine in DMF and shaken for 20 min, then washed.

4.1.3. General procedure for reduction of amide bond

1 M boron–THF solution was added to a flask with pre-swelled resin under nitrogen at 5–10 °C, and the mixture was stirred at 70 °C for 3 h. Excess boron solution was decanted, and the resin was washed four times with methanol, then was immersed in a solution of 0.06 M DBU in MeOH/NMP (1/9) at \sim 5 °C, stirred at room temperature for 6 h, then washed and dried.

4.1.4. General procedure for amide bond formation

The resin bound amine (1 equiv.) was added to a solution of the acids (3 equiv.) and HBTU (3 equiv.) in DMF, followed by addition of DIPEA (3.05 equiv.). The mixture was shaken at 190 rpm for 5 h, then washed and dried. A few beads were taken from each kan selected at random from each pot for a Ninhydrin test and for LC/MS analysis.

4.1.5. General procedure for cleavage from the resin

The products were cleaved from the resin by two 30 min treatments of the kans with 2% TFA in DCM. Solvent was removed using a GeneVac.

4.1.6. Analytical data for representative compounds

6: LC/MS: 96% in ELS, ES[−] 532(M−H), ES⁺ 534(M+H). **7**: LC/MS: 100% in ELS, ES[−] 510(M−H), ES⁺ 512(M+H), 534(M+Na). ¹H-NMR(DMSO-*d*₆) δ 7.89(d, 1H), 7.79(d, 2H), 7.63–7.73(m, 3H), 7.42(t, 2H), 7.33(t, 2H), 4.00–4.30(m, 5H), 3.58(d, 2H), 2.80–2.95(m, 2H), 2.24–2.35(m, 2H), 1.60–1.86(m, 3H), 0.78(d, 6H). **8**: LC/MS: 99.5% in

ELS, ES⁻560 (M–H), ES⁺562(M+H); ¹H-NMR(DMSO-*d*₆) δ 8.94(s, 1H, NH), 8.45(d, 1H), 7.91(d, 2H), 7.75(t, 1H), 7.70(t, 2H), 7.42(t, 2H), 7.33(t, 2H), 7.29(s, 1H), 4.50–4.56(m, 1H), 4.18–4.32(m, 3H), 3.92(q, 1H), 3.15(d, 2H), 2.85–2.96(m, 3H), 2.02–2.20(m, 2H), 1.60–1.80(m, 3H), 0.77(d, 6H). **9**: 100% in ELS, ES⁻592(M–H), ES⁺594(M+H); ¹H-NMR(DMSO-*d*₆) δ 8.53(d, 1H, NH), 7.69–7.92(m, 6H), 7.44(t, 2H), 7.35(t, 2H), 6.93(s, 1H), 4.34–4.50(m, 1H), 4.10–4.40(m, 4H), 2.97–3.02(m, 1H), 2.72–2.90(m, 6H), 1.60–1.65(m, 1H), 0.75(d, 6H). **10**: 100% in ELS, ES⁻624(M–H), ES⁺626(M+H); ¹H-NMR(DMSO-*d*₆) δ 8.58(d, 1H, NH), 7.90(d, 2H, ArH), 7.66–7.71(m, 3H, 2ArH, 1NH), 7.42(t, 2H, ArH), 7.32(t, 2H, ArH), 7.05(s, 1H, ImH), 4.40–4.60(m, 2H), 4.16–4.30(m, 5H), 3.80(t, 1H), 3.56–3.62(m, 1H), 2.80–3.05(m, 4H), 1.59–1.62(m, 1H), 0.73(d, 6H). **11**: LC/MS: 100% in ELS ES⁻548(M–H), ES⁺550(M+H); ¹H-NMR(DMSO-*d*₆) δ 8.48–8.54(m, 2H), 7.84(t, 1H), 7.64(d, 2H), 7.51(d, 2H), 7.41(d, 1H, *J* = 16 Hz), 7.17(s, 1H), 6.74(d, 1H, *J* = 16 Hz), 4.45–4.60(m, 1H), 4.23(q, 1H), 3.10–3.13(m, 1H), 2.88–3.00(m, 3H), 2.05–2.20(m, 2H), 1.70–1.90(m, 3H), 0.78(d, 6H). **12**: LC/MS: 99% in ELS ES⁻623(M–H), ES⁺625(M+H).

4.2. Biochemistry

4.2.1. Preparation of enzyme

E. coli PPAT and Porcine PPAT were prepared by the method described previously [8,9].

4.2.2. Measurement of enzymatic activity

PPAT activity was determined by measuring the production of pyrophosphate [7]. The assay contained 0.53 units PPAT, 80 μM 4-phosphopantetheine derivative *S*-[3'(*N*-propyl)succinamidyl]panthetheine (NPS-pantetheine) and 1 mM ATP in Hepes buffer pH 7.6 and 10% DMSO. Compounds were added to give a final concentration of 50 μM.

4.2.3. Measurement of IC₅₀

IC₅₀ values were calculated from a hypobolic fit of % inhibition vs. compound concentration using origin.

4.3. Crystal structures

The enzyme–inhibitor co-crystals were obtained in the following condition: 19 mg mL⁻¹ *E. coli* PPAT, 2 mM inhibitor, 5% DMSO, 22–32% PEG 8000, 200 mM ammonium sulphate in 100 mM sodium cacodylate buffer at pH 6.0–6.5 at 21 °C. Drop size: 4 μl. Data were collected on Beam line 9.6 of SRS at Daresbury (UK) and on BM14 of the ESRF(France). The protein structure was solved by molecular replacement.

4.3.1. 6/*E. coli* PPAT

This dataset was processed to 2.0 Å in spacegroup C222₁. Overall *R*_{merge} = 9.0%, Completeness = 98.7%, *I*/*σI* = 12.2. Unit cell: *a* = 78.7 Å, *b* = 173.2 Å, *c* = 91.8 Å, α = β = γ = 9°.

4.3.2. 7/*E. coli* PPAT

The data were processed to 2.1 Å in spacegroup *P*3, and were 88.5% complete with an overall *R*_{merge} = 4.2%.

References

- [1] J.D. Robinsaw, J.R. Neely, Am. J. Physiol. 248 (1985) E1–E9.
- [2] Y. Abiko, J. Biochem. 61 (1967) 290–299.
- [3] S. Jackowski, in: F.C. Neidhardt, R. Curtiss, C.A. Gross, J.L. Ingraham, E.C.C. Lin, K.B. Low, W. Reznikoff, M. Riley, M. Schaechter, H.E. Umbarger (Eds.), *Escherichia coli* and *Salmonella typhimurium*, American Society of Microbiology, Washington, DC, 1996, pp. 687–694.
- [4] W. Shaw, A. Lewendon, WO 0017387 A1 990921.
- [5] T. Suzuki, Y. Abiko, M. Shimizu, J. Biochem. 62 (1967) 542–649.
- [6] D.M. Worral, P.K. Tubbs, Biochem. J. 215 (1983) 153–157.
- [7] A. Lewendon, A. Lloyd, WO 0042214 (2000).
- [8] A. Geerlof, A. Lewendon, W.V. Shaw, J. Biol. Chem. 274 (1999) 27105–27111.
- [9] S.T. Ali, A.J. Lloyd, A. Lewendon, Patent, application No: UK02051126 (2002).